ACS Energy LETTERS

http://pubs.acs.org/journal/aelccp

A "Li-Eye" View of Diffusion Pathways in a 2D Intercalation Material from Topochemical Single-Crystal Transformation

Joseph V. Handy, Justin L. Andrews, Saul Perez-Beltran, Daniel R. Powell, Ryan Albers, Luisa Whittaker-Brooks, Nattamai Bhuvanesh, and Sarbajit Banerjee*

Cite This: *ACS Energy Lett.* 2022, 7, 1960−1962

Read Online

ACCESS | Metrics & More | Article Recommendations | Supporting Information

ABSTRACT: We use single-crystal-to-single-crystal transformations to directly image with sub-angstrom resolution distortions of the host lattice, Li site occupancies, and diffusion pathways in a 2D metastable intercalation material. We capture atomistic descriptions of Li-ion diffusion pathways and reconstruct a Li-eye view of available interstitial sites through a 2D intercalation host to address a long-standing challenge in the design of cathode materials and pave the way to atom-precise structural modifications.

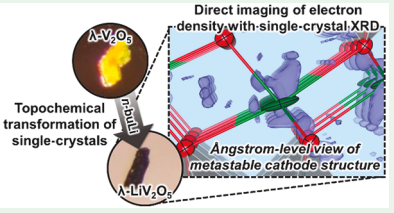

In intercalation electrodes used in energy storage, the insertion of cations and their transport through the crystal lattice bring about a dynamical modulation of structure.[1,2] Capturing atomistic descriptions of these diffusion pathways is critical to the rational design of cathodes.[3−5] *Operando* powder X-ray diffraction (PXRD) is the technique of choice for examining the transformations of electrode materials.[6] However, one-dimensional structure-factor data obtained from PXRD yields limited atomistic information on low-Z atoms such as Li. Since Li cannot be directly imaged, the order in which it occupies specific sites and the diffusion pathways it traverses through host materials remain poorly understood.

A promising strategy for resolving diffusion pathways traversed by Li-ions at the atomic level involves topochemical single-crystal-to-single-crystal transformations.[7,8] However, this approach has found limited use in battery science since single crystals of intercalation cathodes have been difficult to access and intercalate without disintegration. Here, we demonstrate the use of single-crystal XRD (with ∼10^3 more raw reflections as compared to PXRD) to track the topochemical lithiation of macroscopic single crystals to access a new metastable 2D polymorph of V_2O_5, follow the sequence of sites filled by inserted Li-ions, and directly image Li-ions with sub-Å resolution as they diffuse across the 2D host lattice. Through a series of single-crystal-to-single-crystal transformations (Figure 1), we develop a "Li-eye" view of diffusion pathways traversed by Li-ions across an 2D cathode (SI video and Figure 2A). These site preferences are confirmed by electron paramagnetic resonance (EPR) analysis and first-principles DFT studies (Figure 2B−E).

Large crystals of the monoclinic precursor structure ε-$Cu_{0.85}V_2O_5$ (Figure 1A) can be accessed by solid-state methods as described in the Supporting Information (SI). This structure, comprising infinite double layers of VO_6 polyhedra connected by disordered Cu-ions filling 6-coordinate octahedral sites,[9] provides a 2D framework that can be topochemically leached of Cu-ions by oxidation with a solution of $NOBF_4$ in acetonitrile. Cu-ion de-intercalation and corresponding oxidation of V^{4+} to V^{5+} effect a dramatic color change in crystals from black to yellow (Figure 1A−C insets). The metastable, emptied framework is the new polymorph λ-V_2O_5 (Figure 1B), with a dramatically distorted monoclinic angle (124.8° in λ-V_2O_5, compared to 111.6° in ε-$Cu_{0.85}V_2O_5$), corresponding to a substantial shifting of layers but with preservation of V−O connectivity, $C2/m$ space group, and a substantial void space separating the van der Waals bonded layers. The average interlayer distance is indicated by blue dashed arrows in Figure 1A−C. Scanning electron microscopy (SEM) images of large single crystals of λ-V_2O_5 are shown in Figure 1D,E, exhibiting the dramatic exfoliation of the 2D structure and surface cracks induced by strain during de-intercalation. Crystal damage during topochemical treatment introduces disorder, as discussed in detail in the SI, but can be mitigated with the use of mild reaction conditions. The metastable λ-V_2O_5 crystal structure is transformed to the

Received: March 30, 2022
Accepted: May 4, 2022
Published: May 13, 2022

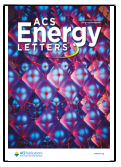

https://doi.org/10.1021/acsenergylett.2c00739
ACS Energy Lett. 2022, 7, 1960−1962

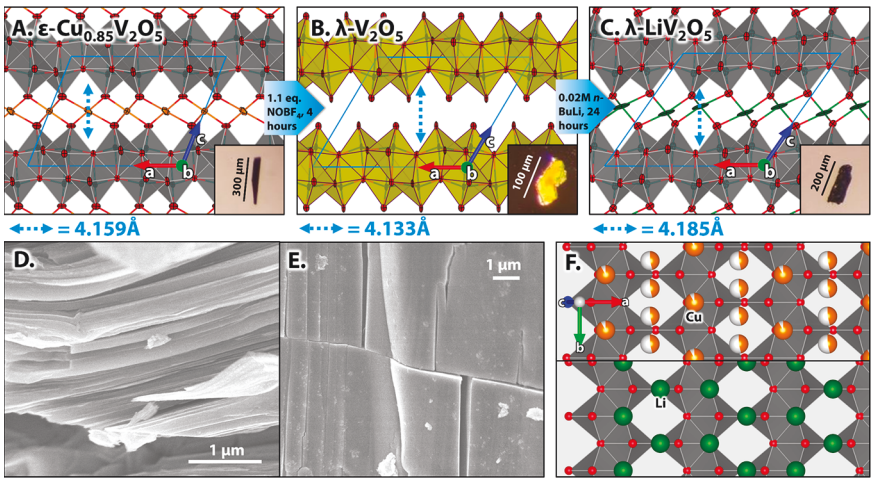

Figure 1. Tracking topochemical single-crystal-to-single-crystal transformations across a novel 2D polymorph of V_2O_5. (A–C) Refined single-crystal structures of pristine ε-$Cu_{0.85}V_2O_5$ (A), leached λ-V_2O_5 (B), and lithiated λ-LiV_2O_5 (C), with inset digital photographs of the single crystals. *C*2/*m* unit cell boundaries are indicated with blue lines, and dashed blue arrows indicate the interlayer separation. Color key: red, O; orange, Cu; green, Li; gray/yellow polyhedra, VO_6. All thermal ellipsoids are shown at 90% probability. (D, E) SEM images of crystals of topochemically leached λ-V_2O_5, showing distinct layers (D) and cracking with preservation of the extended crystal (E). (F) Cutaway view of refined crystal structures viewed down the *c*-axis comparing layer-filling by Cu-ions in pristine ε-$Cu_{0.85}V_2O_5$ (top) and by Li-ions in metastable λ-LiV_2O_5 (bottom).

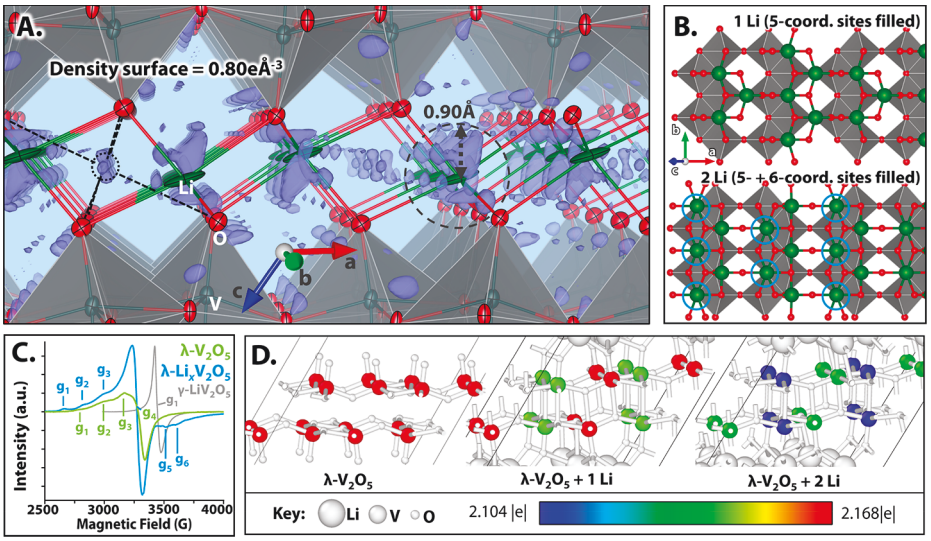

Figure 2. (A) "Li-eye" view of metastable λ-LiV_2O_5, showing the 5-fold coordination of Li between layers of V_2O_5 surrounded by a blue isosurface of residual electron density. One cloud of residual density is circled, and its "coordination environment" is shown with dashed lines; this position corresponds to the 6-coordinate Cu site in the pristine structure. A large dashed circle is used to indicate the Shannon crystal radius of Li (0.90 Å). (B) DFT-calculated structure of empty λ-V_2O_5 with layers populated with 1 Li (top) and 2 Li (bottom) per V_2O_5. (C) EPR spectra of empty (green line) and lithiated (blue line) λ-V_2O_5, with *g*-factors indicated. The EPR spectrum for the thermodynamically stable γ-LiV_2O_5 is also shown as a gray trace, with its single identified *g*-factor indicated. (D) Bader charge analysis of V atoms in λ-V_2O_5, showing increased electron delocalization with Li insertion.

thermodynamic phase α-V_2O_5 between 350 and 400 °C (SI Figure S1).

Topochemical lithiation of λ-V_2O_5 crystals is effected by treatment in dilute *n*-butyllithium solution in heptanes, which leads to a second single-crystal-to-single-crystal transformation to stabilize an entirely new structure, λ-LiV_2O_5 (Figure 1C), with entirely different atomic connectivity as compared to the thermodynamic γ-LiV_2O_5 phase (SI Figure S2).[8] The successful topochemical isolation of λ-LiV_2O_5 represents an important milestone in the development of this technique, which previously has been applied only to crystals of known (albeit metastable) phases of V_2O_5.[7,8] The present work thus attests to the generalizability of these methods for accessing intact single crystals of insertion-type cathodes with extended frameworks capable of continuous distortion, as long as lithiation proceeds slowly enough to prevent mechanical destruction of crystals owing to inhomogeneous strain gradients. Indeed, λ-LiV_2O_5 continues to preserve the overall V_2O_5 lattice inherited from the pristine ε-$Cu_{0.85}V_2O_5$ crystals, but Li-ions fill the highly distorted layers in a new motif, preferring 5-coordinate sites that are highlighted in Figure 1F (see also the SI video). The SI contains detailed crystallographic and single-crystal refinement information (Tables S1–

https://doi.org/10.1021/acsenergylett.2c00739
ACS Energy Lett. 2022, 7, 1960–1962

S6), ICP-MS analyses (Table S7), and PXRD patterns of ground samples (Figure S3).

The high spatial resolution provided by single-crystal XRD allows for viewing the metastable λ-V_2O_5 structure at the level of the individual Li-ions, including thermal disorder of atoms and diffuse electron density indicated by residual structure factor maps (Figure 2A, with a detailed 3D view given in the SI video). The Shannon crystal radius of Li^+ is indicated in Figure 2A with a dashed circle to highlight the void space in these layers available to diffusing Li-ions.[10] DFT calculations for a structure of λ-V_2O_5 populated with 1 Li/V_2O_5 agree well with the site preferences in the experimentally obtained λ-LiV_2O_5 structure (Figure 2B, top panel, compare with Figure 1F, bottom panel). When populated with 2 Li/V_2O_5, the second Li favors the 6-coordinate site occupied originally by Cu in the pristine ϵ-$Cu_{0.85}V_2O_5$ structure (see Figure 1F, top panel) and which is further observed in the difference-density map shown in Figure 2A (this site and its octahedral coordination are indicated with dashed lines), suggesting a site-filling regime whereby Li-ions diffuse down the *b*-axis to first fill 5-coordinate sites and, when those are filled, diffuse in the *a*-direction to fill available 6-coordinate sites to maximize packing in the 2D layers across the *ab* plane. Figure 2C shows EPR spectra for samples of unlithiated λ-V_2O_5 and λ-V_2O_5 treated with 1 equiv of *n*-butyllithium (the relatively smooth spectrum of thermodynamic γ-LiV_2O_5 is also shown for reference), indicating a greater diversity of electronic states with increased lithiation, further suggesting an inhomogeneous site-filling regime. This is reflected in Bader charge analysis (Figure 2D) calculations performed on the λ-V_2O_5 structure across a range of lithiations, indicating the increased dispersion of electrons across V atoms. Crystal orbital Hamiltonian population (COHP) analysis is shown in SI Figure S4.

The ability to access metastable cathode structures as large single crystals allows for structural transformations and Li site-filling behavior to be imaged in unprecedented detail and for reconstruction of a Li-eye view of diffusion pathways. In tandem with crystallographic and spectroscopic information, this paves the way to systematic modification of continuously distorted crystal structures to alter cation diffusion pathways in cathode materials.

■ ASSOCIATED CONTENT

Supporting Information

The Supporting Information is available free of charge at https://pubs.acs.org/doi/10.1021/acsenergylett.2c00739.

Detailed single-crystal structure and refinement information, ICP-MS information, PXRD data, structural comparison to thermodynamic γ-LiV_2O_5, COHP analysis, and experimental details (PDF)

Video exploring infinite 2D layers and Li-ion positions in context with the residual electron density map (MOV)

X-ray crystal data for λ-V_2O_5 (CCDC 2154907) (CIF)

X-ray crystal data for λ-LiV_2O_5 (CCDC 2154908) (CIF)

■ AUTHOR INFORMATION

Corresponding Author

Sarbajit Banerjee − *Department of Chemistry and Department of Materials Science & Engineering, Texas A&M University, College Station, Texas 77843, United States;* orcid.org/0000-0002-2028-4675; Email: banerjee@chem.tamu.edu

Authors

Joseph V. Handy − *Department of Chemistry, Texas A&M University, College Station, Texas 77843, United States*

Justin L. Andrews − *Department of Chemistry, Texas A&M University, College Station, Texas 77843, United States*

Saul Perez-Beltran − *Department of Chemistry, Texas A&M University, College Station, Texas 77843, United States*

Daniel R. Powell − *Department of Chemistry, University of Utah, Salt Lake City, Utah 84112, United States*

Ryan Albers − *Department of Chemistry, Texas A&M University, College Station, Texas 77843, United States*

Luisa Whittaker-Brooks − *Department of Chemistry, University of Utah, Salt Lake City, Utah 84112, United States;* orcid.org/0000-0002-1130-1306

Nattamai Bhuvanesh − *Department of Chemistry, Texas A&M University, College Station, Texas 77843, United States*

Complete contact information is available at: https://pubs.acs.org/10.1021/acsenergylett.2c00739

Notes

The authors declare no competing financial interest.

■ ACKNOWLEDGMENTS

This work was supported by the National Science Foundation under DMR 1809866.

■ REFERENCES

(1) Whittingham, M. S. Ultimate Limits to Intercalation Reactions for Lithium Batteries. *Chem. Rev.* **2014**, *114*, 11414.

(2) De Jesus, L. R.; Andrews, J. L.; Parija, A.; Banerjee, S. Defining Diffusion Pathways in Intercalation Cathode Materials: Some Lessons from V $_2$ O $_5$ on Directing Cation Traffic. *ACS Energy Lett.* **2018**, *3*, 915.

(3) Yao, X.; Zhao, Y.; Castro, F. A.; Mai, L. Rational Design of Preintercalated Electrodes for Rechargeable Batteries. *ACS Energy Lett.* **2019**, *4*, 771.

(4) Bashian, N. H.; Abdel-Latif, S.; Zuba, M.; Griffith, K. J.; Ganose, A. M.; Stiles, J. W.; Zhou, S.; Scanlon, D. O.; Piper, L. F. J.; Melot, B. C. Transition Metal Migration Can. Facilitate Ionic Diffusion in Defect Garnet-Based Intercalation Electrodes. *ACS Energy Lett.* **2020**, *5*, 1448.

(5) Xu, Y.; Wang, Z.; Yang, Z.; Na, J.; Azhar, A.; Wang, S.; Yu, J.; Yamauchi, Y. New Insights into the Lithium-Ion Diffusion Mechanism in Vanadate Compounds. *ACS Energy Lett.* **2021**, *6*, 886.

(6) Luo, Y.; Bai, Y.; Mistry, A.; Zhang, Y.; Zhao, D.; Sarkar, S.; Handy, J. V.; Rezaei, S.; Chuang, A. C.; Carrillo, L.; et al. Effect of Crystallite Geometries on Electrochemical Performance of Porous Intercalation Electrodes by Multiscale Operando Investigation. *Nat. Mater.* **2022**, *21*, 217.

(7) Handy, J. V.; Luo, Y.; Andrews, J. L.; Bhuvanesh, N.; Banerjee, S. An Atomic View of Cation Diffusion Pathways from Single-Crystal Topochemical Transformations. *Angew. Chem., Int. Ed.* **2020**, *59*, 16385.

(8) Handy, J. V.; Andrews, J. L.; Zhang, B.; Kim, D.; Bhuvanesh, N.; Tu, Q.; Qian, X.; Banerjee, S. Topochemical Stabilization and Single-Crystal Transformations of a Metastable 2D γ'-V_2O_5 Intercalation Cathode. *Cell Reports Phys. Sci.* **2022**, *3*, 100712.

(9) Rozier, P.; Dollé, M.; Galy, J. Ionic Diffusion Mastering Using Crystal-Chemistry Parameters: τ-$Cu_{1/2}Ag_{1/2}V_2O_5$ Structure Determination and Comparison with Refined δ-$Ag_xV_2O_5$ and ϵ-$Cu_xV_2O_5$ Ones. *J. Solid State Chem.* **2009**, *182*, 1481.

(10) Shannon, R. D. Revised Effective Ionic Radii and Systematic Studies of Interatomic Distances in Halides and Chalcogenides. *Acta Crystallogr., Sect. A* **1976**, *32*, 751.